This is the Pre-Published Version.

Preparation of TiO_2/ITO and TiO_2/Ti Photoelectrodes by Magnetron Sputtering for Photocatalytic Application

C. He[a], X.Z. Li[a*], N. Graham[a], Y. Wang[b]

[a]*Department of Civil and Structural Engineering, The Hong Kong Polytechnic University, Hong Kong, China*

[b]*Department of Applied Physics, The Hong Kong Polytechnic University, Hong Kong, China*

Abstract

Two types of immobilized TiO_2 films with nanostructure, TiO_2/ITO conductive glass and TiO_2/Ti mesh, were prepared by a radio frequency magnetron sputtering technique, in which a titanium (Ti) target was sputtered in a gaseous mixture of argon and oxygen. The TiO_2 films were characterized by X-ray diffraction, AFM microscopy, SEM microscopy and photoelectrochemical measurements. Their photocatalytic (PC) activity, photoelectrocatalytic (PEC) activity and electrochemical (EC) activity were evaluated in the degradation of 2,4,6-trichlorophenol (TCP) in aqueous solution. The experiments confirmed that the TiO_2 films sputtered at 2.0 Pa had relatively high PC activity due to more active sites formed on the surface of TiO_2 films. The experiments demonstrated that the PEC activity of the TiO_2/Ti mesh was better than that of TiO_2/ITO, resulting from less impedance between the TiO_2 film and Ti mesh. Furthermore, the experiments also demonstrated that at a higher anodic potential, the TiO_2/Ti mesh exhibited not only a PEC reaction but also an EC oxidation reaction at the backed Ti mesh in the degradation of TCP. This study concludes that the sputtered TiO_2 /Ti mesh is an effective photoelectrode for achieving an enhanced TCP degradation in such a PEC reaction system.

Keywords: Photoelectrocatalysis, photoelectrochemistry, Photocatalysis, TiO_2, 2,4,6-trichlorophenol

1. Introduction

*Corresponding author: Tel: +852 2766 6016; Fax: +852 2334 6389, E-mail: cexzli@polyu.edu.hk (X.Z. Li).

Titanium dioxide (TiO_2), as a catalyst in photocatalytic reactions, has been extensively studied for its potential in a variety of environmental applications including the purification of water and wastewater [1-3]. For such a purpose, the removal of persistent organic pollutants (POPs) such as various chlorophenols from industrial wastewater and sewage effluents is of a particular interest [4-6]. At present, TiO_2 is one of the most accepted photocatalysts [7] and it has been widely used as fine powder. However, due to the difficulty of separating these TiO_2 particles from an aqueous phase after wastewater treatment, various TiO_2 films as immobilized TiO_2 catalysts have been prepared by different approaches such as sol-gel techniques, dip-coating methods, and anodic oxidation processes [8-18]. Furthermore, the efficiency of the photocatalytic (PC) oxidation reaction can be further improved by using TiO_2 film electrodes to produce a photoelectrocatalytic (PEC) oxidation reaction [19-24]. In our previous work, a few TiO_2 film electrodes were prepared by either coating TiO_2 onto indium-tin oxide (ITO) conducting glass or electrically anodizing Ti mesh in sulfuric acid solution as photoanodes to be used for the PEC reaction [9,10,21]. Although these TiO_2 films have demonstrated good photoactivity for both PC and PEC reactions, their mechanical stability and electrolyzed dissolution under application of a high electrical potential are still of concern affecting their durability in practical applications. On the other hand, the impedance of electron mass transfer between the TiO_2 film and its supporting media is also a critical factor in the PEC reaction.

Compared to the wet processes, the magnetron sputtering method has some advantages over conventional techniques, which is capable of producing large–scale uniform coatings with a high packing density and strong adhesion [11-17]. Many publications have considered on the sputtering deposition technique, but, up to now, most of them have mainly focused on the film structure relevant to material sciences. To the best of our knowledge, a detailed investigation of the PC and PEC activity of the sputtered TiO_2 film, especially the effect of the supporting medium, has not been reported. In our earlier work, a TiO_2/Ti mesh electrode prepared by anodic oxidation, and a TiO_2/ITO electrode prepared by coating TiO_2 on to the ITO to immobilize TiO_2, were used to investigate the PC and PEC activity [9,10,21]. A study by Dumitriu et al. [13] found that ITO glass as a supporting medium provides the most efficient thin film only in the PC reaction, compared to silicon and alumina supports.

This paper summarises some results of a study aimed at producing a TiO_2 photoelectrode with good durability and high photoactivity for application in water and

wastewater treatment, in which two types of photoelectrodes, TiO_2/ITO film glass and TiO_2/Ti film mesh, were prepared by a magnetron sputtering method. In this work the structural characteristics of the photoelectrodes were examined and their electrochemical and photochemical properties were investigated via the degradation of 2,4,6-trichlorophenol (TCP) in aqueous solution.

2. Experimental section

2.1. Materials

A piece of titanium metal (purity > 99.9% and diameter: 50 mm) was purchased from Superconductive Components Inc. USA and used as a Ti target in the magnetron sputtering system. Titanium mesh (purity > 99.6%, nominal aperture: 0.19 mm, and wire diameter: 0.23 mm) was obtained from Goodfellow Co., U.K. and ITO conductive glass plates with a thickness of 1.3 mm were provided by Shenzhen Nanya Technology Ltd., China. Both the Ti mesh and ITO glass were used as substrate materials to prepare the TiO_2/Ti mesh and TiO_2/ITO glass electrodes, respectively. TCP chemical with a purity of 99.0% was purchased from Aldrich Chemical Co. and used as a model pollutant in the experiment without further purification. TiO_2 powder (P25) was purchased from Degussa Co..

2.2. Preparation of TiO_2/ITO and TiO_2/Ti films

Two types of TiO_2 films were prepared on the ITO glass plates and Ti mesh (TiO_2/ITO and TiO_2/Ti) by a radio frequency magnetron sputtering system (vacuum parts from Lesker, Co., USA, and a power supply from Advanced Energy, Co., USA).

Before sputtering, the substrate materials were carefully cleaned using high purity acetone and methanol, respectively, and then rinsed with deionized water. After the substrate media and Ti target were installed inside the chamber, the magnetron sputtering system was evacuated down to a base pressure $<1.3 \times 10^{-4}$ Pa and the substrate media were heated to the desired temperature before high purity argon (> 99.99%) and oxygen (> 99.9%) gases were introduced into the system at an Ar:O_2 ratio of 9:1 and a gas pressure was maintained constantly. In the meantime, a radio frequency power supply of 13.52 MHz was applied to generate plasma with an energy density of 2.5 J/cm^2 on the target. The magnetron sputtering processes lasted for 2 h, if not

specified, to form TiO_2 films with a thickness of around 150 nm as determined by a surface profiler (KLA-Tencor, USA).

2.3. Preparation of dip-coated TiO_2/ITO

TiO_2/ITO film was prepared according to a procedure described in the literature [8]. Briefly, 40 g TiO_2 was added to 500 ml water and sonicated for 30 min to break up loosely attached aggregates, and then vigorously agitated to form a fine TiO_2 suspension solution. The TiO_2 suspension was loaded on to an ITO glass plate by a dip-casting method, dried for 15 min on a hot plate at 100 °C and then sintered in a muffle furnace at 500°C for 2 h.

2. 4. Characterization of sputtered TiO_2 films

A UV-PC3101PC spectrophotometer (SHIMASZU, Japan) with an integrating sphere (Specular Reflectance ATT.5DEG) was used to record the diffuse reflectance spectra of the samples. The base line correction was done using a calibrated sample of barium sulphate.

X-ray diffraction (XRD) was performed using a diffractometer (Philips, Xpert system) with radiation of a Cu target (K_α, λ = 0.15406 nm) to determine the crystal structure.

Atomic force microscopy (AFM, NanoScope IV instrument) with an RTESP7 Etched Si probe (Tapping) was used to scan the surface structure of the TiO_2/ITO and TiO_2/Ti samples over an area of 2 μm × 2 μm.

SEM images were obtained by a JSM-6330F-mode Field Emission scanning electron microscopy with the secondary electrons detector (JEOL, Japan).

The electrochemical and photochemical measurements were performed in a standard three-electrode assembly consisting of a sputtered TiO_2 electrode as the photoanode, a Pt wire as the cathode and a saturated calomel electrode (SCE) as the reference. A potentiostat (Model CH650, Shanghai) was used to control electrical potentials with reference to the SCE.

2.5. PC and PEC oxidation experiments

Aqueous TCP solution with an initial concentration of 10 mg l^{-1} (0.051 mM) was prepared by dissolving the TCP chemical into distilled water, in which 10 mM Na_2SO_4

was also added as supporting electrolyte.

Both of PC and PEC oxidation experiments were carried out in a photoreactor consisting of two chambers (2.0 cm × 1.1 cm × 8.0 cm each) connected via a salt bridge. Whilst the PC reaction was conducted in one chamber as a photoreactor only, the PEC reaction was performed using both the chambers. An electrical potential was applied between the two electrodes by a potentiostat (EPS 600, Pharmacia Biotech.). An 8-W UV lamp with its main emission at 365 nm was used as a UV source and air bubbling was continuously provided at a flow rate of 30 ml min^{-1} during the reaction. While the TiO_2/ITO or TiO_2/Ti mesh electrode was placed in the photoreactor as the anode, the Pt electrode and SCE were positioned in another chamber as counter and reference electrodes, respectively.

About 10 ml of aqueous TCP solution was used in both the PC and PEC reactions and the pH of the solution was not controlled during the reaction.

2.6. Chemical Analyses

The TCP concentration in aqueous solution was determined by high performance liquid chromatography (HPLC) consisting of a reverse-phase column (Atlantis dC-18, 5 μm 150 × 4.6 mm), a high-pressure pump (Spectrasystem P4000), an autosampler (Spectrasystem AS3000) and a UV detector (Spectrasystem UV6000LP). A mobile phase containing acetonitrile and water at 65%:35% with 0.1% acetic acid was used and a UV detection wavelength of 294 nm was applied. The retention time of the TCP peak under these conditions was recorded at 6.12 min. The concentration of released chloride ion as a product of TCP dechlorination after PC and PEC reactions was determined by ion chromatography (Shimadzu LC－10Atl) with a conductivity detector (Shimadzu CDD－6A). A Shim-pack IC-A1 anion column and a mobile phase containing 2.5 mM phthalic acid and 2.4 mM tris(hydroxymethyl)aminomethane at a flow rate of 1.0 ml min^{-1} were used for chloride separation.

3. Results and discussion

3.1. Surface characteristics of the sputtered TiO_2/ITO and TiO_2/Ti electrodes

A series of nanostructured TiO_2 films were prepared by sputtering either on ITO glass or Ti mesh with the same preparation procedure but at different deposition

temperatures. These sputtered TiO_2 films were first analyzed by XRD and their XRD patterns are shown in Fig. 1. It can been seen that the TiO_2 film deposited at room temperature was mainly amorphous without any diffraction peaks of either anatase or rutile; the TiO_2 film sputtered at 300 °C was partially crystallized with weak diffraction peaks, corresponding to an anatase structure; the TiO_2 films deposited at 450 °C and 500 °C had a crystallized structure with clear diffraction of anatase. These results indicated that the reaction between the Ti particles sputtered from the Ti target and oxygen atoms was promoted by increasing deposition temperature, which is more favorable to crystallization. Furthermore, the TiO_2 film sputtered at 700 °C still showed diffraction of anatase, which means that a phase transfer from anatase to rutile did not occur to any significant extent at a temperature of 700 °C in situ during the sputtering process. These results are consistent with those reported by Hou et al. [16].

The sputtered TiO_2/ITO and TiO_2/Ti films were then examined by AFM and the images are shown in Fig. 2a and b, respectively. The results demonstrated that the surfaces of the sputtered TiO_2 films either on ITO glass or Ti mesh were well structured with compact voids in agreement with other literature reports [11-13,16]. The column-like TiO_2 grains deposited on the ITO glass were found to be about 30 nm at 300 °C, smaller than those on the Ti mesh, although their roughness was quite similar, which was rougher than the amorphous film deposited at room temperature. As the deposition temperature was set at 700 °C, the surface morphology of the sputtered films had changes resulted from the large particles due to the aggregation of actived atoms in the high temperature.

In order to estimate the optical bandgap of the sputtered films, the UV–Vis DRS spectra of the sputtered TiO_2/ITO film were recorded in Fig. 3. It can be found that the onset of DRS was about 394 nm, corresponding to the electron transition from the top of the valence band to the bottom of conduction band. The estimated optical band-gap was 3.15 eV, which is consistent to other researchers' result [18].

3.2. Photoelectrochemical propertier of TiO_2/ITO and TiO_2/Ti electrodes

To study the electrochemical response of the TiO_2/ITO glass or TiO_2/Ti mesh electrodes to the applied potential, cyclic voltammetry (CV) was investigated in 10 mg l^{-1} TCP solution with 0.01 M Na_2SO_4, but without UV illumination. The cyclic voltammograms are shown in Fig. 4. It can be seen that the current response of the TiO_2/ITO electrode was insignificant even at a potential of up to 1.0 V vs. SCE, which

means that no electrochemical oxidation took place. A small cathodic current that appeared at the negative potentials might be associated with the population intrinsic or surface states for electrons [8, 22]. However, for the TiO_2/Ti mesh electrode, an anodic current began to occur at 1.0 V vs. SCE and further increased slowly along with the increase of applied potential. A study by Vinodgopal et al [20] found that the electrochemical oxidation took place at an applied potential of 1.0 V vs. SCE for the degradation of 4-CP with Ti oxide films backed by conductive glass. In our experiment, this anodic peak might be possibly attributed to the electrochemical oxidation reaction of TCP during the process. In fact, the electrochemical oxidation experiment demonstrated that the TCP removal efficiency on TiO_2/Ti mesh was significant (> 10%) upon applying an anodic potential higher than 1.0 V vs. SCE to the TiO_2/Ti mesh electrode without irradiation (vide post). Therefore, under this experimental condition, TCP would be electrochemically oxidized once the anodic potential was higher than 1.0 V vs. SCE.

To study the photocurrent response of the TiO_2/ITO and TiO_2/Ti electrodes to UV irradiation, the photocurrent-voltage measurements were carried out in the same TCP solution with UV illumination in an on-and-off cycle mode. The results are shown in Fig. 5. It can be seen clearly that the photocurrent generation and decay on the TiO_2/ITO electrode (Fig. 5a) were directly synchronous with the UV illumination being applied on and off. Furthermore, the trend of photocurrent increased with the increase of applied potential and gradually reached a maximum photocurrent at an anodic potential of ca. 0.8 V vs. SCE. This indicates that the photogenerated electrons on the TiO_2/ITO electrode could be effectively driven by this anodic potential to the counter electrode, which would be beneficial to charge separation [19]. However, the TiO_2/Ti mesh electrode had a different photoelectrochemistry. At a low potential (< 1.0 V vs. SCE), the generation of photocurrent on the TiO_2/Ti anode was similar to that on the TiO_2/ITO glass electrode. However, at higher voltages (> 1.0 V vs. SCE), the photocurrent increased significantly with the increase of applied potential and gradually reached a maximum. In addition, the baseline also quickly increased under the irradiation-off state conditions. This phenomenon indicates that the generation of electrical current in the dark at > 1.0 V might be caused by several reasons: (i) anodic oxidation of TCP at backed Ti mesh, (ii) electrochemical oxidation of oxygen evolution, and (iii) anodic dissolution of the Ti mesh and/or TiO_2. It is believed that TCP oxidation in the dark would mainly result from the anodic oxidation on the Ti mesh anode at the high potential.

Consequently, two more measurements were conducted to study the patterns of photocurrent generation on the TiO_2/ITO and TiO_2/Ti electrodes versus illumination time at a fixed potential of +0.8 V vs. SCE, respectively. The photocurrent-time profiles for a period of 6 h are shown in Fig. 6. It can be seen clearly that both the TiO_2/ITO and TiO_2/Ti electrodes demonstrated a rapid photocurrent response (either upsurge or dropping off), when the UV illumination was on and off. Both the photocurrents under illumination were maintained at two constant levels throughout the entire experimental period. These results confirmed that these sputtered TiO_2 electrodes behaved photoactive and also gave a steady photoelectrochemical performance under UV illumination. In addition, at the potential of +0.8 V vs. SCE, the photocurrent of the TiO_2/Ti film was about 2 times that of the TiO_2/ITO film. The higher generation of photocurrent on the TiO_2/Ti mesh electrode might result from a better electron transfer rate between the two materials of the TiO_2 film and the Ti supporting mesh so that the photogenerated electrons are more easily transferred out of the film to form a greater current in the external electric field. Therefore, the TiO_2/Ti mesh electrode would have an advantage over the TiO_2/ITO glass electrode for a better performance in a PEC reaction system.

3.3. PC activity of TiO_2/ITO and TiO_2/Ti films

The PC activity of the sputtered TiO_2/ITO and TiO_2/Ti films was evaluated by studying the degradation of TCP in aqueous solution. Since the deposition temperature and total sputtering pressure during the magnetron sputtering are two critical conditions that affect the crystallization and PC activity of the TiO_2 films, two sets of PC oxidation tests were carried out in the TCP solution with an initial concentration of 10 mg l^{-1} and under UV illumination, and using different TiO_2/ITO or TiO_2/Ti films sputtered at different deposition temperatures and total sputtering pressures. All tests lasted for 60 min and the experimental results are shown in Figs 7 and 8.

The experimental results in Fig. 7showed that the deposition temperature had a minor influence on the PC activity of TiO_2/ITO or TiO_2/Ti films. It seems that the TiO_2 films prepared at 500 °C achieved the highest PC activity in the TCP degradation due to good crystallization during sputtering. These results had a good agreement with the XRD and AFM results. It is believed that the high sputtering deposition temperature of 700 °C resulted in the large particles due to the aggregation of atoms could reasonably explain the decreased PC activity. Compared to the TiO_2/ITO films, the PC activity of

TiO_2/Ti films was slightly lower. This might result from a definite nominal aperture of raw Ti mesh.

The experimental results in Fig. 8 demonstrated that the total sputtering pressure also affects the PC activity of TiO_2 films slightly. It can be seen that the PC activity increased with the decrease of total sputtering pressure applied. The TiO_2 films prepared at 2.0 Pa achieved the highest PC activity in the TCP degradation under these experimental conditions. However, any further lower pressure below 2.0 Pa was not investigated in this study. The difference in PC activity can be ascribed to the different surface status of the TiO_2 films prepared at different total sputtering pressures. In general, the sputtering pressure influences the ions arriving to the substrate media during the sputtering process [15]. When the sputtering pressure is high, the ions arriving to the substrate will have lower kinetic energy, leading to the structural defects. It is believed that the TiO_2 films sputtered at 2.0 Pa with relatively higher PC activity resulted from more active sites formed on the surface of TiO_2 films.

3.4. PEC activity of TiO_2/ITO and TiO_2/Ti electrodes

To compare with the PC oxidation reaction, the following experiments were carried out in the two-chamber PEC reaction system, in which a sputtered TiO_2/ITO or TiO_2/Ti electrode was used as the anode and a Pt plate was used as the cathode, and an anodic potential in the range of 0-2.0 V vs. SCE was applied by the potentiostat. Three sets of experiments were performed to degrade TCP in aqueous solution with the same initial concentration of 10 mg l^{-1} but different configurations: (i) TCP oxidation under UV illumination using the TiO_2/ITO electrode; (ii) TCP oxidation under UV illumination using the TiO_2/Ti electrode, and (iii) TCP oxidation in the dark using the TiO_2/Ti electrode.

The experimental results showing the degree of TCP removal are given in Fig. 9a. It can be seen that the degree of TCP removal achieved in such a PEC reaction system was higher than that in the PC reaction system for both the TiO_2/ITO and TiO_2/Ti electrodes. For example, the TCP removal in the PC oxidation using the TiO_2/Ti electrode was 67% after 60 min and the TCP removal in the PEC oxidation at 0.8 V vs. SCE was 79% for the same reaction time. A control experiment was also carried out by applying the same anodic potential of 0.8 V vs. SCE to the TiO_2/Ti electrode but without UV irradiation. The experiment demonstrated that the TCP removal under this condition was insignificant (< 3%), which means that direct oxidation of TCP on the

anode was quite weak due to a low potential of 0.8 V vs. SCE. In fact, this result was also confirmed by the CV curve of TiO_2/Ti electrode as shown in Fig. 4. Therefore, it may be concluded that the externally-applied anodic potential in the PEC reaction system can drive away the accumulated electrons on the TiO_2 photoanode effectively and result in the enhancement of TCP degradation in aqueous solution significantly. In addition, it is noticed that the enhancement of the TCP degradation due to the anodic potential application was more significant for the TiO_2/Ti electrode (12%) than that for the TiO_2/ITO electrode (7%), comparatively. This might be the result of a better electron mass transfer rate on the TiO_2/Ti mesh than that on the TiO_2/ITO glass, since the TiO_2 film had a lower impedance with Ti metal rather than ITO conductive glass.

According to the CV results shown in Fig. 4, it is known that the electrochemical oxidation of TCP on the Ti electrode under this experimental condition needs an anodic potential of at least 1.0 V vs. SCE, which further confirmed that the enhancement of TCP degradation in the potential range of 0-0.8 V vs. SCE mainly resulted from the PEC oxidation. Fig. 9a also showed the results of TCP removal at a higher potential range from 0.8 to 2.0 V vs. SCE, since some reports have indicated that the PEC activity can be improved to a greater extent at a higher potential [23, 24]. From the results in Fig. 9a, it can be confirmed that the TCP removal increased with the increase of anodic potential in both cases using a TiO_2/ITO and a TiO_2/Ti electrode, but the improvement using the TiO_2/Ti electrode was significantly greater than that using the TiO_2/ITO electrode, especially at the higher potential range beyond 1.0 V vs. SCE. It is believed that the further improvement of TCP degradation at the higher potential range resulted mainly from the electrochemical oxidation reaction on the backed Ti mesh anode, which has been demonstrated by the results in the third set of experiments also shown in Fig. 9a.

These results had a good agreement with the results of photocurrent-voltage responses of TiO_2/ITO in our previous work [9,10]. However, for the TiO_2/Ti mesh electrode, it can be seen that the TCP removal increased with the increase of anodic potential significantly over the whole range of anodic potential 0-2.0 V. In order to investigate the contribution of the electrochemical oxidation to the TCP removal, a series of blank experiments were carried out by applying an anodic potential in the range of 0.3-2.0 V in the dark. The experiment demonstrated that the electrochemical oxidation of TCP on backed Ti anode was not negligible where there was an anodic potential greater than 1.0 V. From the results of the enhancement effect of PEC compared to the PC process (Fig. 9b) the anodic potential of 0.8 V vs. SCE was found

to be the optimal potential.

The TCP removal in the various reactor systems, that is, the TiO_2/ITO electrode or the TiO_2/Ti mesh electrode in PC and PEC processes, is summarised in Fig.10. The experimental data were found to fit approximately a first-order kinetic model, $\ln(C_0/C_t) = f(t)$ [25,26], and the values of the kinetic constant, k, are listed in Table 1. The reaction rates for the 4 processes can be ranked from high to low as (D) > (C) > (B) > (A). Although the PC activity of TiO_2/Ti mesh was lower than that of TiO_2/ITO, the PEC reaction rate using TiO_2/Ti mesh electrode was higher than TiO_2/ITO at the same anodic potential. During the TCP degradation, a dechlorination reaction is one of the important steps to reduce the toxicity of the pollutant [27,28]. As a final product of the dechlorination reaction, chloride ion was analyzed at different reaction times and the results are also shown in Fig. 10. It can be seen that the dechlorination reaction was systematic and consistent with the TCP degradation reaction. The experimental results indicated that the chloride production during the TCP degradation in the PEC system using the TiO_2/Ti mesh (65% dechlorination) was significantly higher than that of using TiO_2/ITO (48% dechlorination). This further confirmed that the photoactivity of the TiO_2/Ti mesh in the PEC reaction system was better than the TiO_2/ITO electrode

3.5. Durability of photoelectrodes

For the practical application of such a PEC reaction process, not only the photocatalytic activity of a photoelectrode is important, but its durability or lifetime is also critical. Since many photoelectrodes are prepared by various dip-coating techniques, they have difficulty in being applied in practical applications due to their limited lifetime. Alternatively, the TiO_2/ITO and TiO_2/Ti electrodes prepared by the magnetron sputtering technique in this study had a high packing density and strong adhesion. Both of them were tested (in the PEC system) for their ability to degrade TCP in aqueous solution for a series of 10 identical tests. Their performances were evaluated and are shown in Fig. 11. It can be seen that while the coated TiO_2/ITO electrode demonstrated a slight decline of its effectiveness from 83% to 75% of TCP degradation after 10 repeated uses, the sputtered TiO_2/ITO and TiO_2/Ti mesh electrodes retained their degradation effectiveness at 78% and 80%, respectively, within the limits of experimental error. Furthermore, SEM images of the coated TiO_2/ITO and sputtered TiO_2 electrodes were also examined before and after the 10 repeated tests and examples of these are presented in Figs. 12 and 13, respectively. It can be seen clearly that the

coated TiO_2/ITO film after use showed some apparent cracks and less uniformity than before use (Fig. 12). However, the sputtered TiO_2 electrodes appeared to display no significant changes before and after use (Fig. 13). These results indicate that the mechanical strength and durability of the sputtered TiO_2 film is much better than that of the coated TiO_2 film, and this would be a significant advantage of the use of sputtered TiO_2 film in practice.

4. Conclusions

Both types of TiO_2 films with high uniformity were successfully prepared on Ti mesh by a magnetron sputtering technique and on conventional conducting glass by a dip-coating technique. Their photoactivities were evaluated in PC and PEC systems in terms of the degradation of TCP in aqueous solution. The experiments demonstrated that while the PC activity of the TiO_2/ITO film was slightly higher than that of the TiO_2/Ti film, the PEC activity of the TiO_2/Ti mesh was significantly better than that of TiO_2/ITO. Furthermore, the sputtered TiO_2 electrodes demonstrated better durability during repeated tests than the coated TiO_2/ITO film. However, from the view of enhanced PEC activity compared to PC, it may be concluded that the sputtered TiO_2 /Ti mesh is an effective photoelectrode for application in a PEC reaction system and which has the advantage of a greater durability.

Acknowledgements

The authors wish to thank the University Grants Committee of the Hong Kong Government for financial support for this work (RGC No: PolyU5148/03E) and also thank the Guangdong National Natural Science Foundation (Project No. 04011602).

References

1. M.R. Hoffman，S.T. Martin，W.Y. Choi, D.W. Bahnemann, Chem. Rev. 95 (1995) 69-96.
2. A. Fujishima, T.N. Rao, A. Tryk, J. Photochem. Photobiolo. C: Photochem. Rev. 1 (2000) 1-21.
3. G. Ceńti, P. Ciambelli, S. Perathoner, P. Russo, P., Catal. Today 75 (2002) 3-15.
4. J. Peller, O. Wiest, P.V. Kamat, Environ. Sci. Technol. 37 (2003) 1926-1932.
5. C.C. Chen, P.X. Lei, H.W. Ji, W.H. Ma, J.C. Zhao, H. Hidda, N. Serpone, Environ. Sci. Technol. 38 (2004) 329-337.
6. E. Kusvuran, A. Samil, O.M. Atanur, Appl. Catal. B 58 (2005) 211-216.

7. R. Morand, C. Lopez, M. Koudelka-Hep, P. Kedzierzawski, J. Augustynski, J. Phys. Chem. B 106 (2002) 7218-7224.
8. K. Vinodgopal, S. Hotchandani, P.V. Kamat, J. Phys. Chem. 97 (1993) 9040- 9044.
9. C. He, Y. Xiong, J. Chen, C.H. Zha, X.H. Zhu, J. Photochem. Photobiol, A 157 (2003) 71-79.
10. C. He, X.Z. Li, N. Graham, Y. Xiong, J. Appl. Electrochem. 35 (2005) 741-750.
11. M. Gomez, J. Rodriguez, S.E. Lindquist, Thin Solid Films 342 (1999) 148-152.
12. J. Rodriguez, M. Gomez, J. Ederth, G.A. Niklasson, C.G. Granqvist, Thin Solid Films 365 (2000) 119-125.
13. D. Dumitriu, A.R. Bally, C. Ballif, P. Hones, P.E. Schmid, R. Sanjines, F. Levy, V.I. Parvulescu, Appl. Catal. B 25 (2000) 83-92.
14. P. Zeman, S. Takabayashi, Thin Solid Films 433 (2003) 57-62.
15. S.K. Zheng, G. Xiang, T.M. Wang, F. Pan, C. Wang, W.C. Hao, Vacuum 72 (2003) 79-84.
16. Y.Q. Hou, D.M. Zhuang, G. Zhang, M. Zhao, M.S. Wu, Appl. Sur. Sci. 218 (2003) 97-105.
17. C.H. Heo, S.B. Lee, J.H. Boo, J.H., Thin Solid Film 475 (2005) 183-188.
18. T. Sasaki, N. Koshizaki, J.W. Yoon, K.M. Beck, J. Photochem. Photobiolo. A: Chem. 145 (2001) 11-16.
19. D.H. Kim, M.A. Anderson, M.A., 1994. Environ. Sci. Technol. 28 (1994) 479-483.
20. K. Vinodgopal, U. Stafford, K.A. Gray, P.V. Kamat, J. Phys. Chem. 98 (1994) 6797 – 6803.
21. X.Z. Li, H.L. Liu, P.T. Yue, Y.P. Sun, Environ. Sci. Technol. 34 (2000) 4401-4406.
22. M.V.B. Zanoni, J.J. Sene, M.A. Anderson, J. Photochem. Photobiol. A 157 (2003) 55-63.
23. T.C. An, Y. Xiong, G.Y. Li, C.H. Zha, X.H. Zhu, J. Photochem. Photobiol. A 152 (2002) 155-165.
24. T.C. An, G.Y. Li, X.H. Zhu, J.M. Fu, G.Y. Sheng, Z. Zhu, Appl. Catal. A 279 (2005) 247-256.
25. X.Z. Li. F.B. Li, F.B., Environ. Sci. Technol. 35 (2001) 2381-2387.
26. C. He, Y. Xiong, C.H. Zha X.H. Zhu, J. Chem. Tech. Biotech. 78 (2003) 717-723.
27. M. Hugul, E. Ercag, R. Apak, J. Environ. Sci. Health. A 37 (2002) 365-383.
28. Y.C. Chen, P. Smirniotis, P., Ind. Eng. Chem. Res. 41 (2002) 5958-5965.

Table 1. The values of kinetic coefficient *k* in four experiments with application of the first-order kinetic model

ID	Catalyst	Process	Rate constant *k* (min^{-1})	Correlation coefficient (R)
A	TiO_2/ Ti mesh	PC	0.02135	0.97244
B	TiO_2/ ITO	PC	0.02511	0.95197
C	TiO_2/ITO	PEC	0.03036	0.95466
D	TiO_2/Ti mesh	PEC	0.03195	0.94685

List of figure captions

Fig. 1. XRD patterns of sputtered TiO_2/ITO at different deposition temperature: (a) room temperature; (b) 300 °C; (c) 400 °C; (d) 450 °C; (e) 500 °C, and (f) 700 °C.

Fig. 2. AFM images of (a) sputtered TiO_2/ITO and (b) sputtered TiO_2/Ti mesh at different deposition temperatures of 300 °C, 500 °C, and 700 °C, respectively.

Fig. 3. UV-Vis DRS of sputtered TiO_2/ITO film (Deposition temperature = 500 °C; total gas pressure = 2.0 Pa, and oxygen partial pressure = 0.2 Pa).

Fig. 4. Cyclic voltammograms of 10 mg l^{-1} TCP in 0.01 M Na_2SO_4 without illumination for (a) sputtered TiO_2/ITO and (b) sputtered TiO_2/Ti mesh (Deposition temperature = 500 °C; total gas pressure = 2.0 Pa, and oxygen partial pressure = 0.2 Pa).

Fig. 5. Photocurrent-voltage curves for the TCP oxidation under chopped light of (a) sputtered TiO_2/ITO and (b) sputtered TiO_2/Ti mesh (Deposition temperature = 500 °C; total gas pressure = 2.0 Pa, and oxygen partial pressure = 0.2 Pa. The inset in 4(b) is an enlargement of the photocurrent-voltage curves scanning the range 0-1.46 V vs. SCE.

Fig. 6. Stability of the photocurrent of (a) sputtered TiO_2/ITO and (b) sputtered TiO_2/Ti mesh with the O_2 flow rate of 30 mL min^{-1} (Deposition temperature = 500°C; total gas pressure = 2.0 Pa; and oxygen partial pressure = 0.2 Pa).

Fig. 7. Effect of deposition temperature on TCP degradation performance (Total gas pressure = 2.0 Pa, and oxygen partial pressure = 0.2 Pa).

Fig. 8. Effect of total gas pressure on TCP degradation performance (Deposition temperature = 500°C).

Fig. 9. Effect of applied anodic potential on (a) TCP removal performance and (b) TCP removal enhancement of PEC compared to PC (Deposition temperature = 500°C; total gas pressure = 2.0 Pa; and oxygen partial pressure = 0.2 Pa).

Fig. 10. Comparison of TCP degradation (solid symbols) and released chloride (open symbols) under different process systems (initial concentration in all case of 10 mg l^{-1}, the anodic potential of 0.8 V vs. SCE in the PEC process, sputtered TiO_2 film was deposited at 500 °C and the total gas pressure of 2.0 Pa with oxygen partial pressure of 0.2 Pa).

Fig. 11. Variation of TCP removal on the number of batch runs for the two TiO_2 film types (initial TCP concentration in all cases was 10 mg l^{-1}, an anodic potential of 0.8 V vs. SCE, and sputtered TiO_2/Ti film was deposited at 500 °C and the total gas pressure of 2.0 Pa with oxygen partial pressure of 0.2 Pa.).

Fig. 12. SEM micrographs of dip-coating TiO_2 film (a) before, and (b) after, the tenth runs of the PEC process at 0.8 V vs. SCE.

Fig. 13. SEM micrographs of sputtered TiO_2/Ti mesh deposited at 500 °C and the total gas pressure of 2.0 Pa with oxygen partial pressure of 0.2 Pa. (a) before, and (b) after, the tenth runs of the PEC process at 0.8 V vs. SCE.

Fig. 1

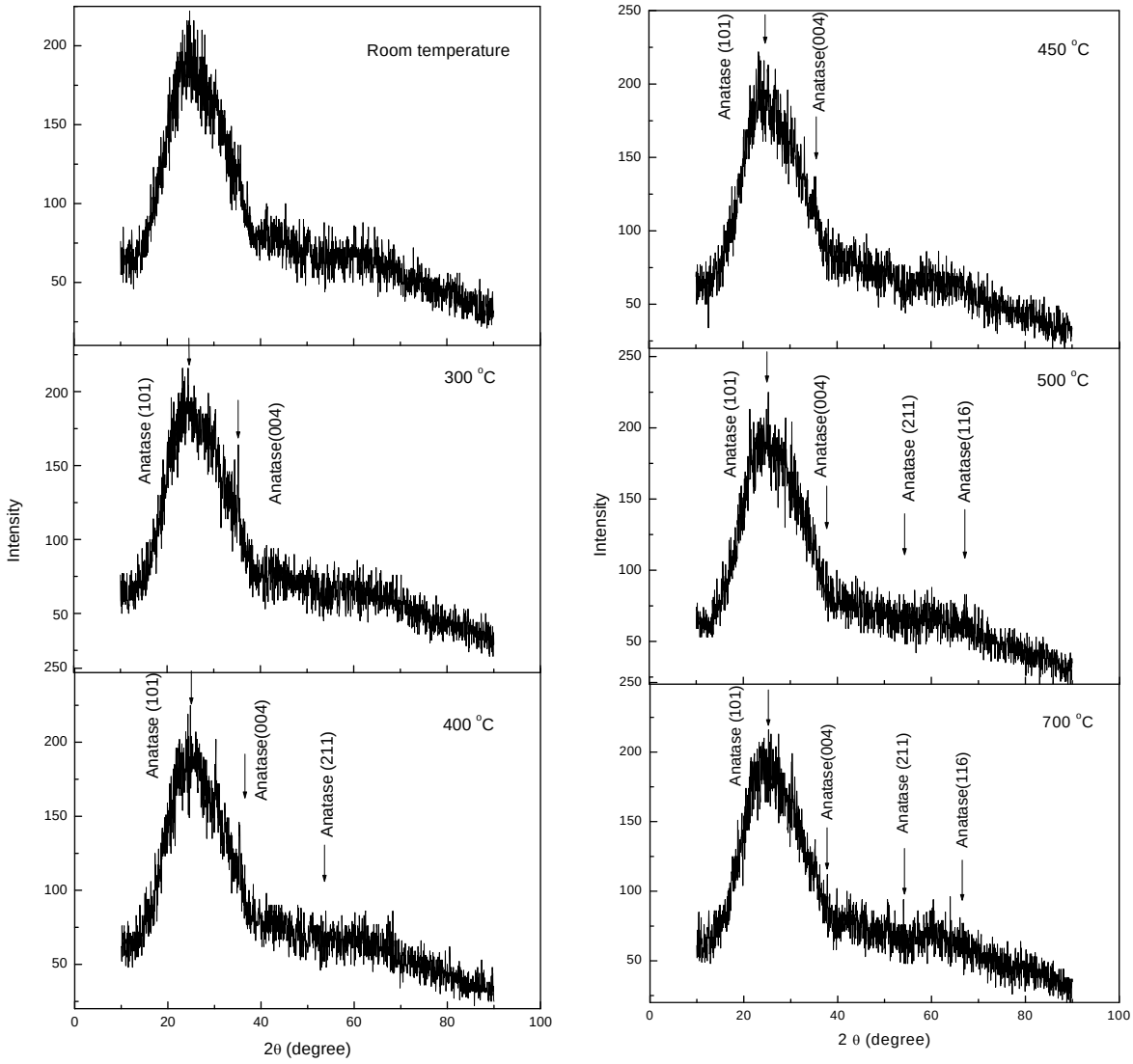
Room temperature
300 °C
400 °C
450 °C
500 °C
700 °C
Anatase (101)
Anatase(004)
Anatase (211)
Anatase(116)
Intensity
2θ (degree)
2 θ (degree)

Fig. 2.

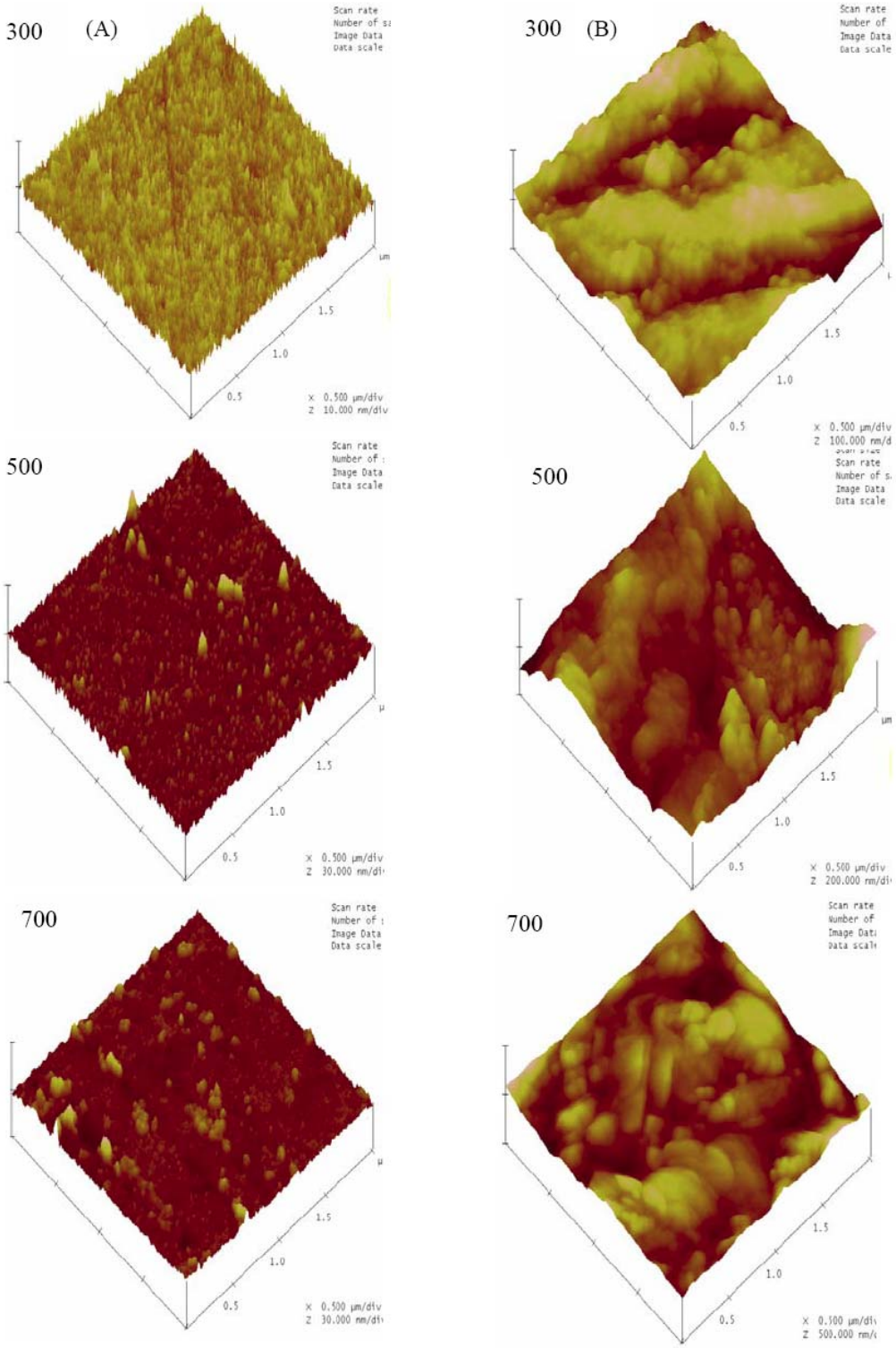
300
(A)
Scan rate
Image Data
Data scale
1.5
1.0
0.5
x 0.500 µm/div
z 10.000 nm/div
300
(B)
Scan rate
Number of
Image Data
Data scale
1.5
1.0
0.5
x 0.500 µm/div
z 100.000 nm/d
500
Scan rate
Number of :
Image Data
Data scale
1.5
1.0
0.5
x 0.500 µm/div
z 30.000 nm/di
500
Scan rate
Number of s.
Image Data
Data scale
1.5
1.0
0.5
x 0.500 µm/div
z 200.000 nm/di
700
Scan rate
Number of :
Image Data
Data scale
1.5
1.0
0.5
x 0.500 µm/div
z 30.000 nm/di
700
Scan rate
Number of
Image Dat
Data scale
1.5
1.0
0.5
x 0.500 µm/di
z 500.000 nm/

Fig. 3

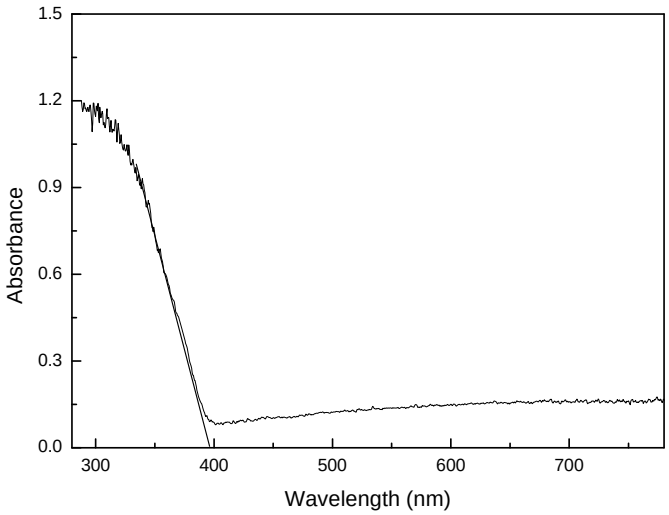

Fig. 4

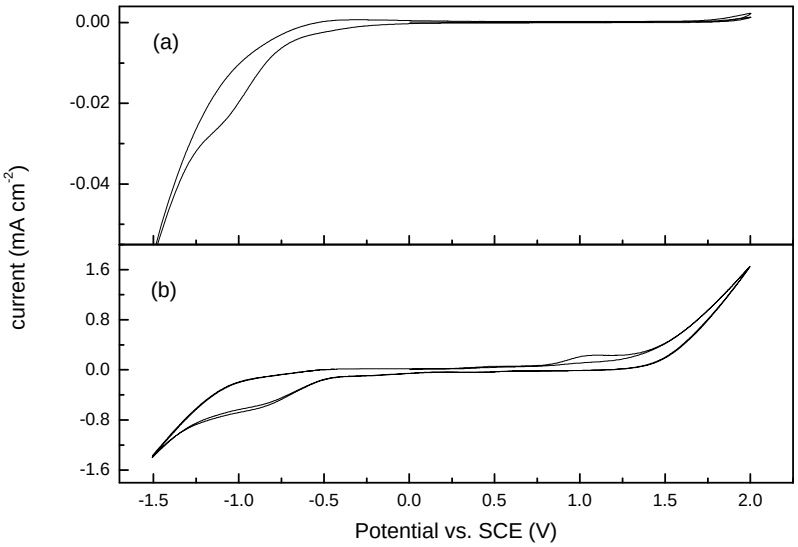
0.00
-0.02
-0.04
(a)
1.6
0.8
0.0
-0.8
-1.6
(b)
current (mA cm-2)
-1.5
-1.0
-0.5
0.0
0.5
1.0
1.5
2.0
Potential vs. SCE (V)

Fig.5

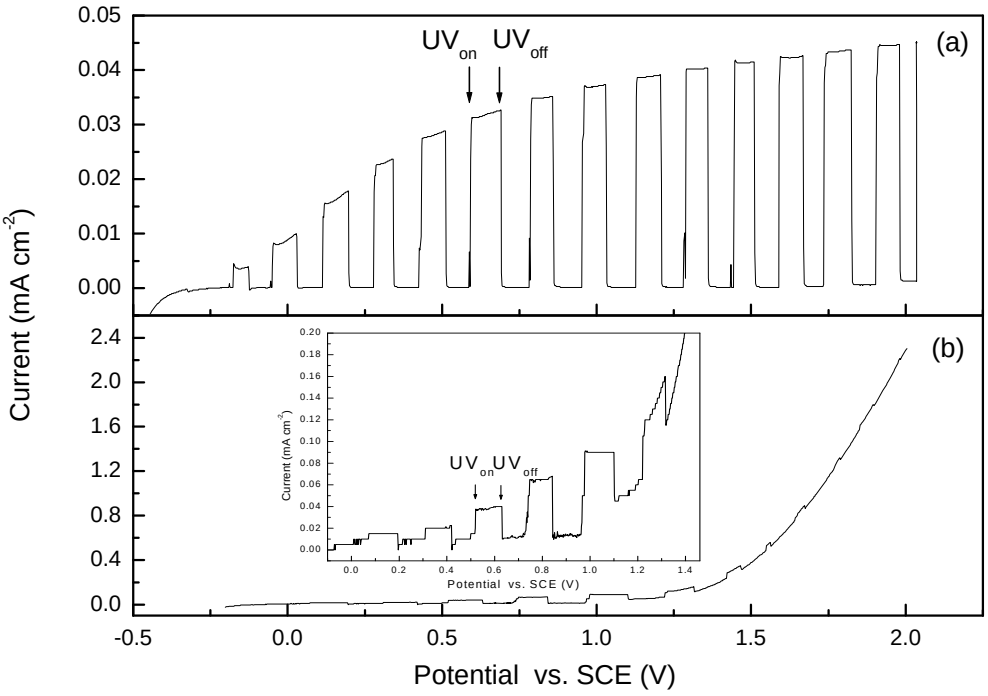
UV_on
UV_off
(a)
(b)
Current (mA cm^-2)
Potential vs. SCE (V)
0.05
0.04
0.03
0.02
0.01
0.00
2.4
2.0
1.6
1.2
0.8
0.4
0.0
-0.5
0.0
0.5
1.0
1.5
2.0
0.20
0.18
0.16
0.14
0.12
0.10
0.08
0.06
0.04
0.02
0.00
0.0
0.2
0.4
0.6
0.8
1.0
1.2
1.4

Fig. 6

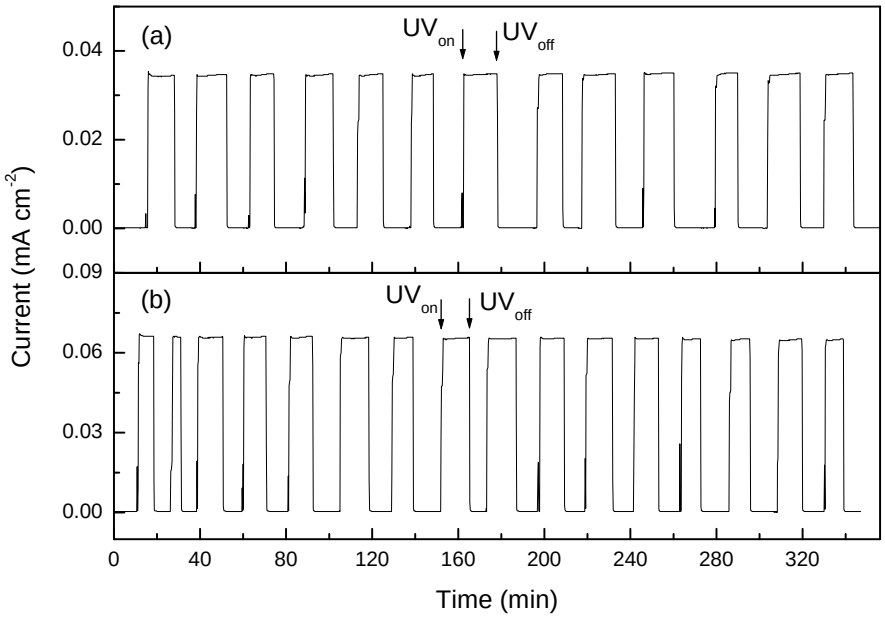
(a)
UV on
UV off
0.04
0.02
0.00
0.09
(b)
UV on
UV off
0.06
0.03
0.00
Current (mA cm-2)
0
40
80
120
160
200
240
280
320
Time (min)

Fig. 7.

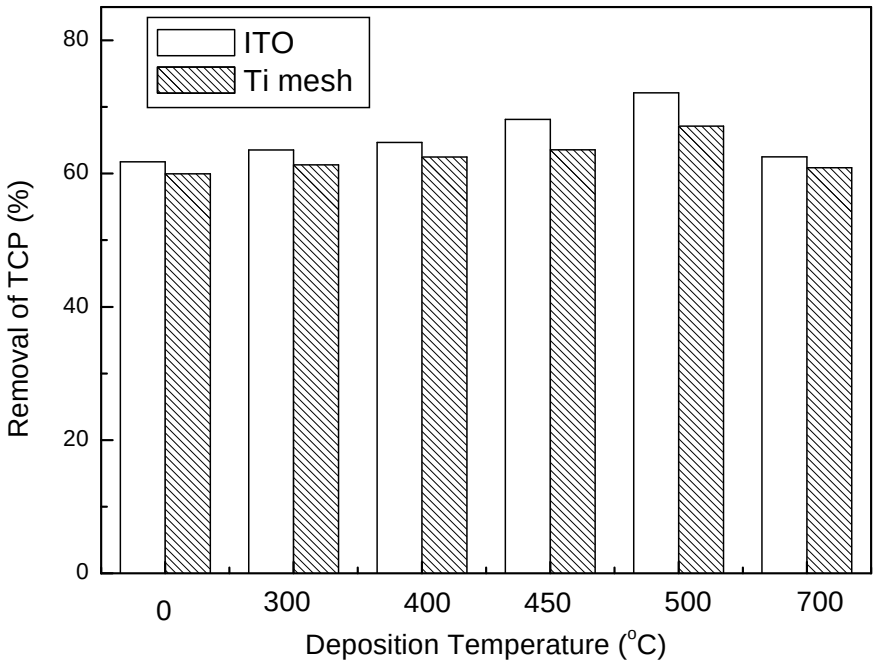
ITO
Ti mesh
Removal of TCP (%)
0
20
40
60
80
0
300
400
450
500
700
Deposition Temperature (°C)

Fig. 8.

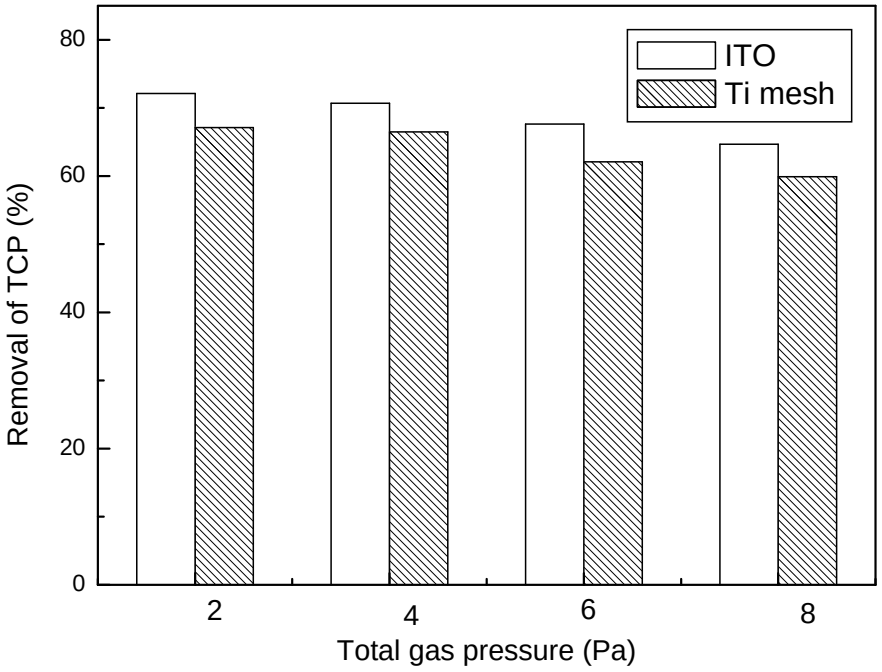
ITO
Ti mesh
Removal of TCP (%)
0
20
40
60
80
2
4
6
8
Total gas pressure (Pa)

Fig. 9

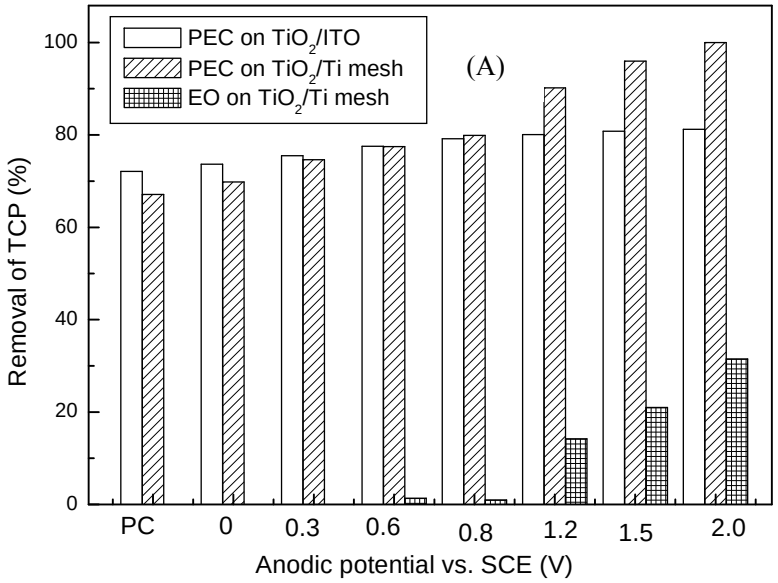
PEC on TiO2/ITO
PEC on TiO2/Ti mesh
EO on TiO2/Ti mesh
(A)
Removal of TCP (%)
0
20
40
60
80
100
PC
0
0.3
0.6
0.8
1.2
1.5
2.0
Anodic potential vs. SCE (V)

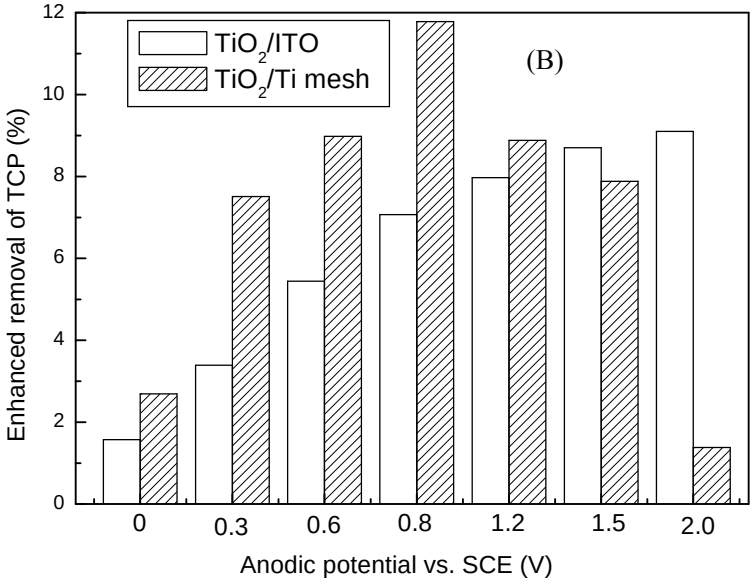
TiO2/ITO
TiO2/Ti mesh
(B)
Enhanced removal of TCP (%)
0
2
4
6
8
10
12
0
0.3
0.6
0.8
1.2
1.5
2.0
Anodic potential vs. SCE (V)

Fig. 10

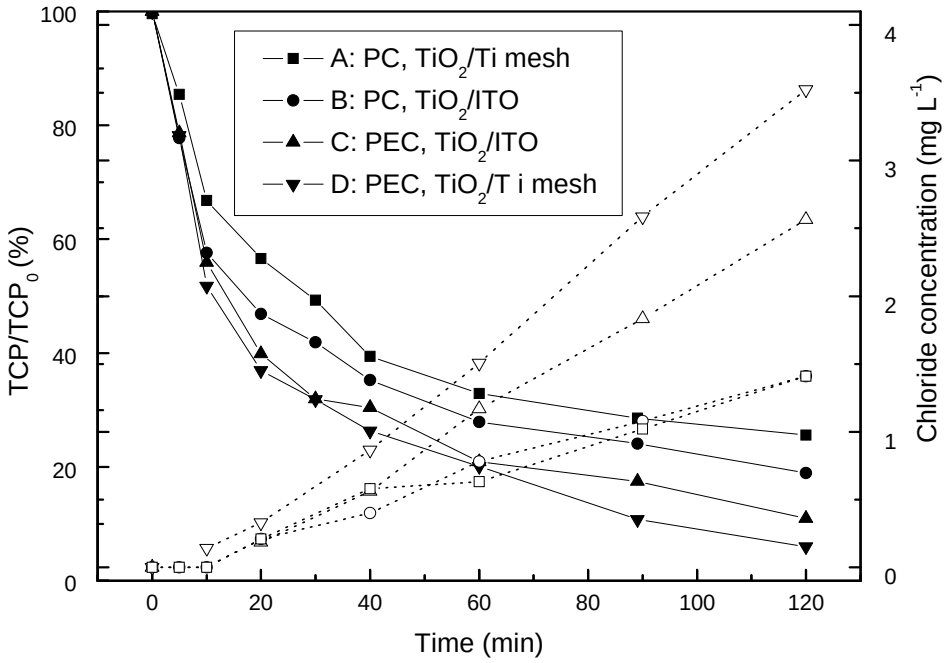
A: PC, TiO2/Ti mesh
B: PC, TiO2/ITO
C: PEC, TiO2/ITO
D: PEC, TiO2/T i mesh
TCP/TCP0 (%)
Chloride concentration (mg L-1)
Time (min)
0
20
40
60
80
100
120
0
1
2
3
4

Fig. 11

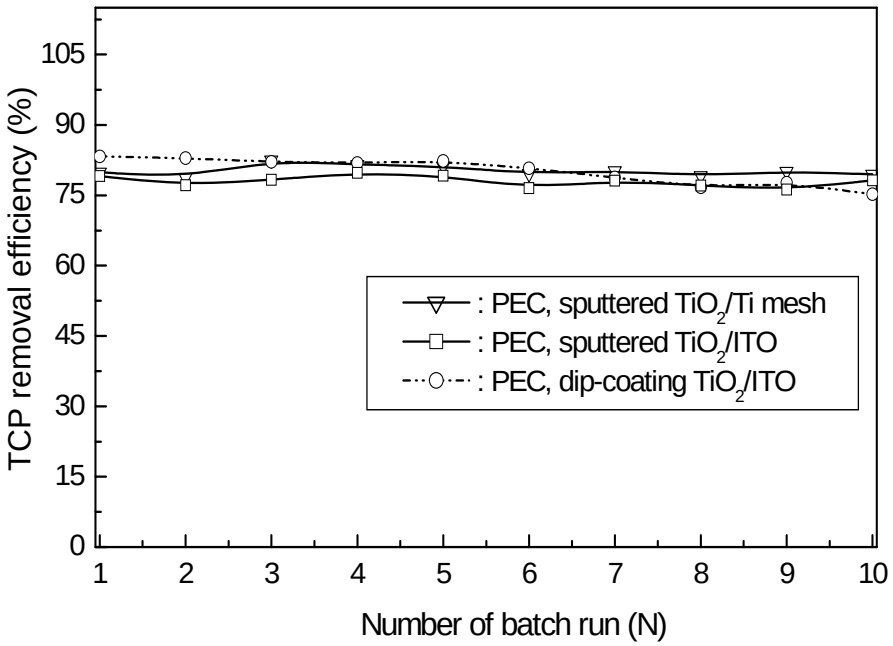
TCP removal efficiency (%)
105
90
75
60
45
30
15
0
1
2
3
4
5
6
7
8
9
10
Number of batch run (N)
: PEC, sputtered TiO2/Ti mesh
: PEC, sputtered TiO2/ITO
: PEC, dip-coating TiO2/ITO

Fig. 12

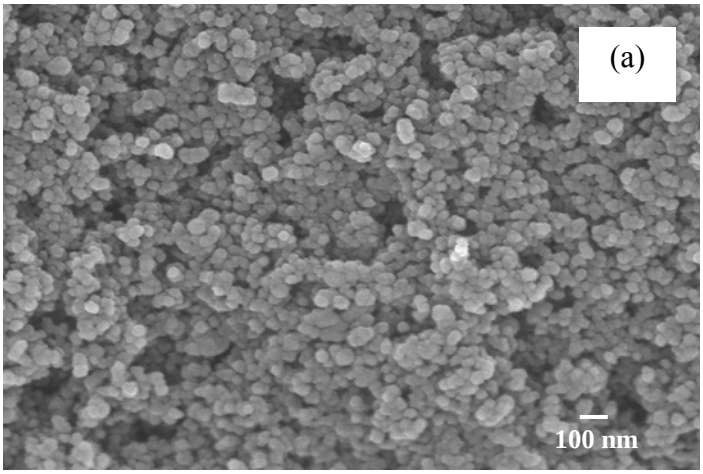

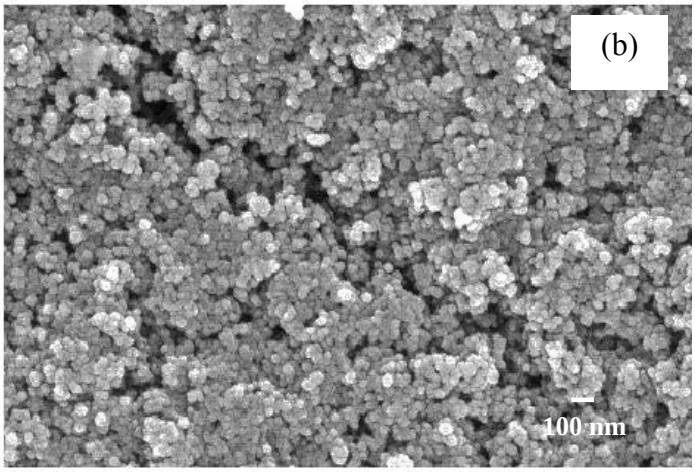
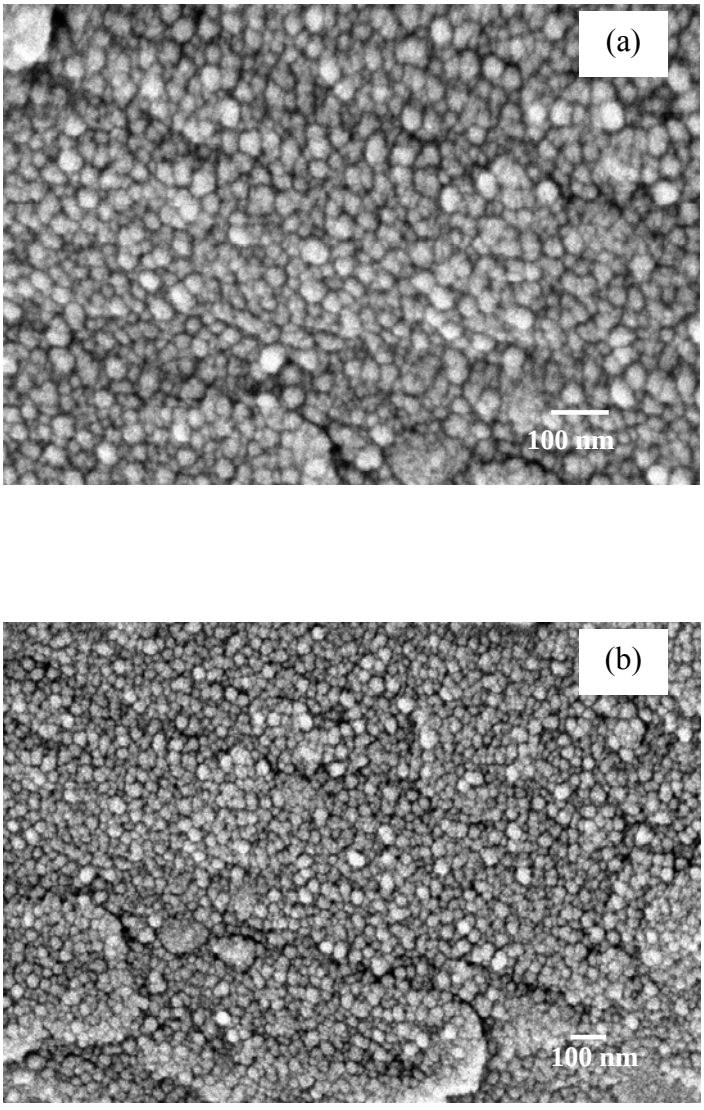
Fig. 13